

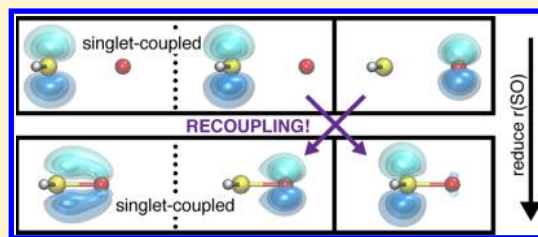
# Bonding in Sulfur–Oxygen Compounds—HSO/SOH and SOO/OSO: An Example of Recoupled Pair $\pi$ Bonding

Beth A. Lindquist, Tyler Y. Takeshita, David E. Woon, and Thom H. Dunning, Jr.\*

Department of Chemistry, University of Illinois at Urbana–Champaign, 600 S. Mathews Avenue, Urbana, Illinois 61801, United States

## S Supporting Information

**ABSTRACT:** The ground states ( $X^2A''$ ) of HSO and SOH are extremely close in energy, yet their molecular structures differ dramatically, e.g.,  $r_e(\text{SO})$  is 1.485 Å in HSO and 1.632 Å in SOH. The SO bond is also much stronger in HSO than in SOH: 100.3 kcal/mol versus 78.8 kcal/mol [RCCSD(T)-F12/AVTZ]. Similar differences are found in the  $\text{SO}_2$  isomers, SOO and OSO, depending on whether the second oxygen atom binds to oxygen or sulfur. We report generalized valence bond and RCCSD(T)-F12 calculations on HSO/SOH and OSO/SOO and analyze the bonding in all four species. We find that HSO has a shorter and stronger SO bond than SOH due to the presence of a recoupled pair bond in the  $\pi(a'')$  system of HSO. Similarly, the bonding in SOO and OSO differs greatly. SOO is like ozone and has substantial diradical character, while OSO has two recoupled pair  $\pi$  bonds and negligible diradical character. The ability of the sulfur atom to form recoupled pair bonds provides a natural explanation for the dramatic variation in the bonding in these and many other sulfur–oxygen compounds.



## I. INTRODUCTION

Peculiarities abound in the chemistry of the main group elements in the second (Al–Ar) and subsequent rows of the periodic table. For example, the HSO and SOH isomers differ little in energy (just 4.2 kcal/mol<sup>1</sup>), yet the SO bond lengths in the two isomers differ by 0.14 Å,<sup>1</sup> and as we will show, the S–O bond energies differ by more than 21 kcal/mol. In a similar vein, the reactivities of sulfur dioxide ( $\text{SO}_2$ ) and ozone ( $\text{O}_3$ ) differ dramatically despite the similarities in the description of the electronic structure of these two molecules given in many chemistry texts.<sup>2</sup> Clearly, there are gaps in our understanding of the fundamental factors that control molecular structure, energetics and reactivity in the main group elements beyond the first row.

In previous papers,<sup>3–9</sup> our research group found that a new type of chemical bond—the *recoupled pair bond*—accounts for many of the differences in the properties of molecules containing the late p-block elements of the first and subsequent rows of the periodic table. A recoupled pair bond differs from a covalent bond in that it involves three electrons. For two atoms to form a recoupled pair bond, the electron in a singly occupied orbital forms a bond with an electron that was a member of a lone pair on the other atom. In the case of the late p-block elements, the  $p^2$  lone pair of electrons can be uncoupled from one another to form a bond with an incoming ligand. Recoupled pair bond energies, while smaller than the corresponding covalent bonds, can still be significant, especially when the element containing the lone pair is in the second row or beyond and when the ligand is very electronegative.

The ability of elements such as sulfur to form recoupled pair bonds with halides explains:

- the occurrence of hypervalent species of second row elements, such as  $\text{SF}_4$  and  $\text{SF}_6$ , which do not exist for the first row elements
- the presence of excited states in compounds of second row elements that are either only weakly bound or absent in the corresponding first row compounds, e.g., the  $\text{SF}(^4\Sigma^-)$  state
- the dramatic variations in sequential bond energies in second row compounds such as in  $D_e(\text{F}_{n-1}\text{S–F})$ ,  $n = 2–6$
- the edge mechanism for molecular inversion in heavily halogenated tricoordinated species of the second row elements
- reactions involving compounds of the second row elements that have no correspondence in compounds of the first row elements.

For an overview of the above, see ref 4.

There is great interest in the chemistry of inorganic sulfur–oxygen compounds because of their importance in atmospheric chemistry, organic chemistry, battery electrolytes, and many other applications.<sup>10–12</sup> For example, HSO and SOH have garnered much theoretical and experimental consideration because HSO is thought to catalyze ozone depletion.<sup>11,13–15</sup> In this and a subsequent paper, we will show that recoupled pair bonding explains the anomalies noted above in HSO versus SOH, OSO versus SOO (this paper), and  $\text{O}_3$  versus  $\text{SO}_2$  (the following paper). The recoupled pair bonds in all of our previous studies were in  $\sigma$  systems, but it is also possible to

Received: July 24, 2013

Published: August 15, 2013



form recoupled pair bonds in  $\pi$  systems. Recoupled pair  $\pi$  bonds affect the structures, the energetics, and ultimately, the reactivity of these molecules. In this paper, we will illustrate the impact of recoupled pair bonds in  $\pi$  systems by comparing a number of properties of HSO versus SOH and OSO ( $\text{SO}_2$ ) versus SOO. The former pair of compounds arises from the addition of a monovalent species (H) to SO, the latter pair from an addition of a divalent species (O) to SO.

The remainder of the paper is organized as follows. In section II, the computational methodology will be discussed. In section III, the electronic structure of the  $^3\Sigma^-$  ground state of SO will be examined. We will illustrate the impact of recoupled pair  $\pi$  bonding by comparing the  $X^2A'$  and  $A^2A'$  states of HSO and SOH in section IV. In section V, we will discuss the analogous comparison of OSO ( $\text{SO}_2$ ) and SOO. Section VI will summarize our conclusions.

## II. COMPUTATIONAL METHODOLOGY

Valence bond (VB) theory is a theoretical framework that describes chemical bonding in terms of atomic orbitals. Unlike molecular orbital (MO) theory, VB wave functions display the correct behavior upon dissociation and thus are well suited for describing bond making and breaking processes. However, the atomic orbitals are typically not allowed to change as a function of nuclear geometry in a VB calculation. Therefore, in order to describe the often-substantial changes in the atomic orbitals caused by molecular formation, many structures corresponding to both covalent and ionic states must be included in the VB calculation, which can complicate the analysis of bonding in the molecule. Another strategy for overcoming this issue is to optimize the VB orbitals self-consistently for each nuclear geometry. The resulting wave function is called a generalized valence bond (GVB) wave function, although it is referred to as a spin-coupled valence bond (SCVB) wave function by others.<sup>16,17</sup> The GVB wave function contains only one orbital structure, which facilitates the interpretation of the calculation.

The GVB wave function for an atom or molecule is

$$\Psi_{\text{GVB}} = \hat{a}\phi_{d1}\phi_{d1} \dots \phi_{dn_d}\phi_{dn_d}\phi_{a1}\phi_{a2} \dots \phi_{an_a}\alpha\beta \dots \alpha\beta\Theta_{S,M}^{n_a} \quad (1)$$

where  $n_d$  is the number of doubly occupied core and valence orbitals,  $n_a$  is the number of singly occupied active orbitals, and  $\Theta_{S,M}^{n_a}$  is a linear combination of the spin functions for the  $n_a$  active electrons with a given total spin ( $S$ ) and spin projection ( $M$ ). The spin functions represent the different ways the spins of the electrons in the active orbitals can be coupled. When describing bond formation, both the orbitals and the coefficients of the spin couplings change as the internuclear distance decreases from those appropriate for the atoms (or fragments) to those appropriate for the molecule.

GVB theory differs from MO theory in that the active orbitals ( $\phi_{ai}$ ) are singly occupied and allowed to be non-orthogonal (the active GVB orbitals are orthogonal to the doubly occupied core and valence orbitals,  $\phi_{di}$ , which are also orthogonal to each other). The computational cost grows rapidly with the number of nonorthogonal singly occupied orbitals and spin functions. Traditionally, the perfect pairing (PP) and strong orthogonality (SO) constraints were invoked to minimize the computational cost.<sup>18</sup> In the PP spin function, the pairs of electrons are singlet coupled, each with a spin function of  $1/\sqrt{2}(\alpha\beta - \beta\alpha)$ :  $\phi_{a1}$  is paired with  $\phi_{a2}$ ,  $\phi_{a3}$  is paired with  $\phi_{a4}$ , etc. with any remaining unpaired electrons coupled as appropriate for the given spin state ( $S, M$ ). In the PP

approximation, only this spin function is included in the calculation. In the SO approximation, the nonsinglet paired orbitals in the PP wave function are forced to be orthogonal. Improvements in computational power and mathematical algorithms have enabled *full* GVB calculations to be performed for many chemical species. In this work, we will present the results of both types of GVB calculations: GVB(SO/PP) and full GVB.

All calculations were performed with the Molpro suite of quantum chemical programs.<sup>19</sup> The GVB calculations were performed using the fully variational CASVB program of Cooper and co-workers<sup>20</sup> with Kotani spin functions.<sup>21</sup> Only the valence  $a''(\pi)$  orbitals, as well as the SO  $\sigma$  bond in HSO and SOH, were included as active orbitals in the GVB calculations, and orthogonality between the  $\sigma$  and the  $\pi$  orbitals was enforced. Initial guesses for the GVB orbitals were derived from a CASSCF wave function with the same active space.<sup>22,23</sup> The explicitly correlated coupled cluster program in Molpro, RCCSD(T)-F12 with the “a” approximation, was used to perform all coupled cluster calculations in this work.<sup>24–27</sup> Explicitly correlated methods can more efficiently represent the exact electronic wave function by including terms that depend explicitly on the interelectronic distance. A calculation with an explicitly correlated methodology and a triple-zeta basis set typically has an accuracy comparable to that from a quadruple or quintuple zeta basis set without the explicitly correlated terms.<sup>28</sup> Triple-zeta correlation consistent basis sets were used for all calculations reported herein [aug-cc-pVTZ<sup>29,30</sup> on hydrogen and oxygen and aug-cc-pV(T+d)Z<sup>31</sup> on sulfur].

We use GVB orbital diagrams to schematically represent the electronic configurations and wave functions of the molecules of interest. In these diagrams, the three p orbitals of sulfur and oxygen are depicted as follows: the two p orbitals in the plane of the paper are drawn as two lobes; the p orbital that points out of and behind the plane of the paper is drawn as a small circle. The dots represent the electron occupations of the p orbitals. The hydrogen atom is depicted as a circle with a dot (electron) at the center, representing the 1s orbital; see Figure 1. We will introduce additional notation in the following section appropriate for representing bonding of recoupled sulfur  $\pi$  orbitals.

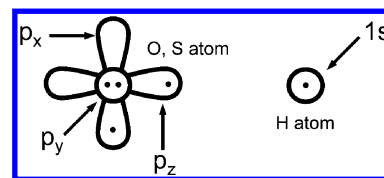


**Figure 1.** GVB orbital diagrams for the sulfur, oxygen, and hydrogen atoms.

## III. THE GROUND $X^3\Sigma^-$ STATE OF SO

**A. The MO Description of Bonding in SO.** The ground state of SO has  $^3\Sigma^-$  symmetry. The singlet states,  $^1\Delta$  and  $^1\Sigma^+$ , arising from the  $\pi^2$  configuration lie at higher energies, in accordance with Hund's Rule.<sup>32</sup> The calculated equilibrium bond energy and bond length of  $\text{SO}(X^3\Sigma^-)$  are  $D_e = 125.2$  kcal/mol and  $r_e = 1.483$  Å [RCCSD(T)-F12/AV(T+d)Z], which compare well with the experimental values of  $D_e = 125.2$  kcal/mol and  $r_e = 1.4933$  Å.<sup>33</sup> This bond length is substantially shorter than would be anticipated for a single bond based on

the sum of the covalent radii of the S and the O atoms (1.71 Å),<sup>34</sup> suggesting a contribution from the  $\pi$  electrons to bonding in SO. The orbital diagrams, including the  $\pi$  electrons, for the Hartree–Fock (HF) configuration of  $\text{SO}(X^3\Sigma^-)$  are given in Figure 2a, where the singly occupied orbitals are triplet coupled.

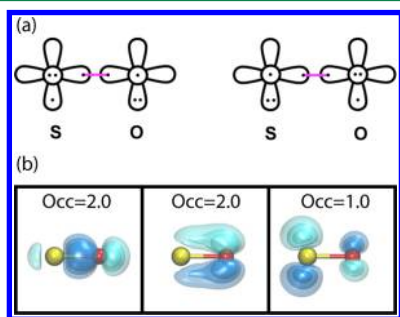


**Figure 2.** (a) Orbital diagrams for the Hartree–Fock (HF) configuration of  $\text{SO}(X^3\Sigma^-)$  and (b) select localized HF orbitals. Throughout the paper, the location of the oxygen atoms is depicted by a red sphere and that of the sulfur atom by a yellow sphere.

Both of these resonance structures contribute equally to form a  $\Sigma$  state. The localized HF orbitals are shown in Figure 2b. As expected, the  $\pi_x$  and  $\pi_y$  orbitals are equivalent due to symmetry; only the  $\pi_x$  orbitals are shown. (The  $\sigma$  orbitals were localized to remove mixing of the  $\sigma$  bond with the valence  $s^2$  pairs of oxygen and sulfur.) In MO theory, bonding in the  $X^3\Sigma^-$  state of SO is described by three doubly occupied bonding orbitals (one  $\sigma$  and two  $\pi$ ) and two singly occupied antibonding orbitals (both  $\pi$ ). Therefore, each  $\pi$  system has a bond order of 1/2. However, this does not mean that the two  $\pi$  systems within each resonance structure ( $\text{S}3p^2$  aligned with  $\text{O}2p^1$  and  $\text{S}3p^1$  aligned with  $\text{O}2p^2$ ) contribute equally to the bonding. In fact, the discrepancies between the molecular structure and energetics of HSO and SOH described in the Introduction are suggestive that these two  $\pi$  systems are in fact not equivalent, with the bonding present in HSO ( $\text{S}3p^2$  aligned with  $\text{O}2p^1$ ) making the largest contribution. In section IV, we will show that recoupled pair  $\pi$  bonding explains why this is the case. However, in order to properly describe recoupled pair bonding, we need to use the GVB wave function.

**B. The GVB Description of the Sulfur and Oxygen Atoms.** To lay the groundwork for describing the GVB diagrams for SO, we will first discuss the GVB orbitals for the sulfur and oxygen atoms. The ground state HF configuration of the sulfur atom is  $3s^2 3p_x 3p_y^2 3p_z$ . The corresponding GVB wave function has the configuration  $3s^2 3p_x 3p_{y-} 3p_{y+} 3p_z$ , i.e., the  $3p_y^2$  lone pair orbital is described by a pair of singlet-coupled  $3p$  lobe orbitals,  $(3p_{y-}, 3p_{y+})$ . As we will show, these lobe orbitals play a significant role in the formation of recoupled pair  $\pi$  bonds. The sulfur lobe orbitals are a mixture of  $3p$  and  $3d$  orbitals,  $c_1 3p \pm c_2 3d$ ; however, this  $3d$  orbital is not identical to the sulfur atomic  $3d$  orbital, and its contribution to the wave function ( $c_2$ ) is small. Plots of the sulfur  $3p\pi$  lobe orbitals relevant to this study, where the  $d$  orbital is the  $3d_{yz}$  orbital, are shown in Figure 3a. Although the  $(3p_{y-}, 3p_{y+})$  lobe orbitals are polarized away from one another (a result of the angular correlation provided by the inclusion of  $3d$  orbital in the wave function), the overlap of the orbitals is still very high (0.89), a fact that limits the type of recoupled pair bonds that can be formed; see ref 4.

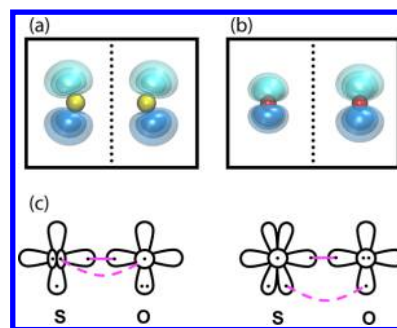


**Figure 3.** (a) GVB  $3p\pi$  lobe orbitals,  $(3p_{y-}, 3p_{y+})$ , for the ground state of the sulfur atom ( $^3P$ ). (b) GVB  $2p\pi$  lobe orbitals,  $(2p_{y-}, 2p_{y+})$ , for the ground state of the oxygen atom ( $^3P$ ). Throughout this work, a dashed line between a pair of GVB orbitals like that separating the sulfur lobes and the oxygen lobes denotes that these orbitals are singlet coupled. (c) Proposed GVB diagrams for the two resonance structures of  $\text{SO}(X^3\Sigma^-)$ .

In contrast to the sulfur atom, the GVB  $(2p_{y-}, 2p_{y+})$  orbitals for the oxygen atom involve excitation into the  $3p_y$  orbital rather than a  $3d$  orbital. One of these GVB orbitals is concentrated near the nucleus, while the other orbital is more diffuse (radial correlation); see Figure 3b. Prior studies of the OF radical have demonstrated that it is much more difficult to form a recoupled pair bond with oxygen—a consequence of both the in–out nature of the  $(2p_{y-}, 2p_{y+})$  GVB orbitals and the more tightly bound nature of the electrons in these orbitals.<sup>8</sup>

**C. The GVB Description of Bonding in  $\text{SO}(X^3\Sigma^-)$ .** In previous works on recoupled pair bonding, two trends were observed: (1) only very electronegative ligands can recouple a  $p^2$  electron pair, and (2) the  $3p^2$  pair of sulfur is much easier to recouple than the  $2p^2$  pair of oxygen.<sup>8</sup> Therefore, we would predict that the  $\pi$  system that aligns the  $3p\pi^2$  orbital on sulfur and the  $2p\pi^1$  orbital of oxygen might form a recoupled pair bond. The converse  $\pi$  system containing a  $3p\pi^1$  sulfur orbital and a  $2p\pi^2$  oxygen orbital is not likely to do so. With these guidelines in mind, we propose GVB orbital diagrams for  $\text{SO}(X^3\Sigma^-)$  in Figure 3c, where the electrons of the sulfur  $3p^2$  pair are represented by two lobes like those plotted in Figure 3a, each containing one electron. The recoupled pair bond between the singly occupied  $2p$  oxygen orbital and one of the lobes on the sulfur atom is indicated with a pink dashed line. Because we do not expect the  $2p^2$  GVB orbitals of oxygen to be recoupled, we depict it as a doubly occupied orbital in the diagrams, though we do allow the  $2p$  electrons to occupy two lobe orbitals in the GVB calculations.

The above description is consistent with the HF orbitals shown in Figure 2b, where the doubly occupied  $\pi$  orbitals are concentrated on the oxygen atom, with some polarization or delocalization toward the sulfur atom. The singly occupied  $\pi$  orbitals are concentrated on the sulfur atom but have a high degree of antibonding character. This indicates that the electrons in these orbitals interact strongly with the electrons in the doubly occupied  $\pi$  orbital with which they are aligned, which would be expected if a recoupled pair bond were present in the  $\pi$  system. However, because the  $\pi$  orbitals are identical due to symmetry, it is not possible to directly observe the differences between the two  $\pi$  systems—one with a recoupled pair  $\pi$  bond and the other without such a bond. In order to circumvent this difficulty, we can add a hydrogen atom to SO to form HSO or SOH. This will lift the symmetry constraints and



enable us to observe any recoupled pair  $\pi$  bonding between S and O.

#### IV. RESULTS FOR THE HSO AND SOH ISOMERS

The ground states of HSO and SOH are both  $X^2A''$  states; GVB orbital diagrams of their formation from H and SO are shown in Figure 4. At the RCCSD(T)-F12/AV(T+d)Z level of

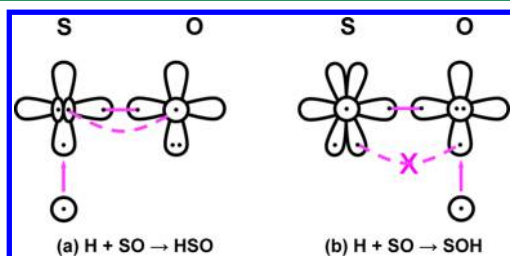


**Figure 4.** GVB orbital diagrams depicting the formation of ground state (a) HSO and (b) SOH from H + SO. In HSO( $X^2A''$ ), the recoupled pair  $\pi$  bond is not broken, but it is in SOH( $X^2A''$ ).

theory without zero-point corrections, the two species are a mere 1.9 kcal/mol separated in energy, with HSO being the more stable species. This near energetic degeneracy is surprising, given the disparate inherent strengths of an OH bond and an SH bond. For instance, the  $^2\Pi$  ground states of OH and SH have dissociation energies of 107.1 and 87.5 kcal/mol, respectively. Therefore, if the SO bond is unaffected by hydrogen addition, we would expect SOH to be approximately 20 kcal/mol more stable than HSO. However, as the GVB diagrams for the two additions show, adding a hydrogen atom to either the sulfur or the oxygen atom of SO is fundamentally different if there is a recoupled pair  $\pi$  bond in the SO molecule. Bond formation with the oxygen atom would disrupt any S–O recoupled pair  $\pi$  bond, weakening that bond. By contrast, bond formation with the sulfur atom will not have a direct effect on the recoupled pair  $\pi$  bond, and so we would expect the S–O bond to be relatively unaffected.

**A. Structures and Energetics of HSO and SOH.** The  $X^2A''$  state of HSO has an S–O bond length ( $r_e$ ) of 1.485 Å and an S–O bond energy ( $D_e$ ) of 100.3 kcal/mol; see Figure 5. In the formation of the  $X^2A''$  state of HSO from  $H(^2S) + SO(X^3\Sigma^-)$ , the hydrogen atom adds to the singly occupied  $3p\pi$  orbital of sulfur. As expected from the preceding analysis, formation of the H–S bond has a modest effect on the S–O bond: its length is essentially unchanged compared to  $SO(X^3\Sigma^-)$  (1.485 Å versus 1.483 Å). The S–O bond in HSO is weaker than that of SO by 24.9 kcal/mol, which can be largely attributed to the additional repulsive pair–pair interactions between the electrons in the SH bond and the oxygen lone pair and SO bond pairs.

In forming the  $X^2A''$  state of SOH from  $H(^2S) + SO(X^3\Sigma^-)$ , the hydrogen atom is added to the  $2p\pi$  orbital of oxygen. As illustrated in Figure 4, this would disrupt an in-plane recoupled pair bond in the  $\pi$  system of  $SO(X^3\Sigma^-)$  if it were present. Indeed, the SO bond is dramatically affected by the formation of the OH bond (Figure 5). In the SOH( $X^2A''$ ) state,  $r_e(\text{SO})$  is 1.632 Å, and the SO bond energy falls to just 78.8 kcal/mol! The bond lengthens by 0.149 Å and weakens by 46.4 kcal/mol relative to  $SO(X^3\Sigma^-)$ , changes far greater than those that occur in the formation of HSO. Formation of the OH bond substantially weakens the SO bond in SOH, as would be

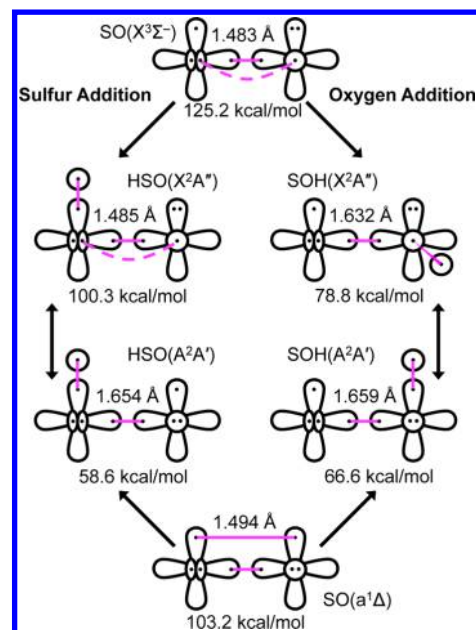


**Figure 5.** Changes in the SO bond lengths and bond energies upon the addition of a hydrogen atom to the SO ( $X^3\Sigma^-$ ) state (top), excitation from the  $X^2A''$  state to the  $A^2A'$  state (middle), and comparison to the  $SO(a^1\Delta)$  state of SO (bottom).

expected if the hydrogen atom was disrupting a recoupled pair  $\pi$  bond.

The results for the ground state of HSO and SOH are consistent with our expectations based on Figure 4. We can further test this conclusion by examining the first excited  $A^2A'$  states of both isomers. The  $A^2A'$  states arise from the  $SO(a^1\Delta)$  state rather than the  $SO(X^3\Sigma^-)$  state. This state contains one covalent bond in one  $\pi$  system and four electrons in the other  $\pi$  system; see Figure 5. Thus, there can be no recoupled pair bonding in  $SO(a^1\Delta)$ . In Figure 5, we compare the  $X^2A''$  states of HSO and SOH to the corresponding  $A^2A'$  states. In the  $A^2A'$  states, both the  $3p\pi$  and  $2p\pi$  orbitals are doubly occupied, removing the possibility of recoupled pair bonding in these states of either HSO or SOH. The two S–O bond energies are relatively weak but similar, 58.6 kcal/mol (HSO) and 66.6 kcal/mol (SOH). These bond energies are much less than in the  $SO(a^1\Delta)$  state, 103.2 kcal/mol, because the  $\pi$  bond in  $SO(a^1\Delta)$  is broken in both cases to form the bond with the H atom. Additionally, because the  $A^2A'$  states do not contain recoupled pair bonds, their relative energies are much closer to expectations based on the inherent strengths of OH and SH bonds; i.e. the OH bond is 19.6 kcal/mol stronger than the SH bond in the diatomic species. The  $A^2A'$  state of SOH is 27.5 kcal/mol more stable than the  $A^2A'$  state of HSO.

For SOH, the  $A^2A'$  state is only 12.3 kcal/mol higher in energy than the  $X^2A''$  state, and the S–O bond is weakened by essentially the same amount. The S–O bond length increases by a modest 0.027 Å relative to the ground state. By contrast, in the case of HSO, the  $A^2A'$  state is 41.7 kcal/mol higher in energy than the  $X^2A''$  state! In addition,  $r_e(\text{SO})$  is 0.169 Å longer in the  $A^2A'$  state. From the results summarized in Figure 5, it is clear that HSO( $X^2A''$ ) is very different than the other three HSO/SOH species and states. In the  $X^2A''$  state of HSO, the recoupled pair  $\pi$  bond shortens and strengthens the S–O bond with respect to the HSO( $A^2A'$ ) state and the SOH  $X^2A''$  and  $A^2A'$  states.

**B. Analysis of GVB Wave Functions and Orbitals for HSO and SOH.** The energetics of SOH and HSO strongly suggest that recoupled pair bonding influences the electronic structure of these species. Further evidence for the formation of recoupled pair bonds can be gleaned from a detailed examination of the GVB  $a''(\pi)$  orbitals in the  $X^2A''$  states of HSO and SOH. In the previous section, we analyzed the effects of adding a hydrogen atom to  $SO(X^3\Sigma^-)$ . However, to observe the changes in the GVB orbitals and spin couplings that accompany recoupled pair bond formation, we will consider the alternative formation pathways,  $HS(^2\Pi) + O(^3P) \rightarrow HSO(X^2A'')$  and  $S(^3P) + OH(^2\Pi) \rightarrow SOH(X^2A'')$ . In the first reaction, we expect O to induce recoupling in the out-of-plane  $\pi$  pair on HS, while in the other case, we do not expect S to be able to recouple the analogous pair of electrons on OH. To ensure no bias, we will describe all valence  $a''$  orbitals with singly occupied GVB orbitals.

It is instructive to first examine the GVB orbitals for SOH, where a recoupled pair  $\pi$  bond is *not* thought to be present. For SOH at  $r(\text{SO}) = r_e(\text{SO}) + 1.0 \text{ \AA}$ , shown in Figure 6a, the

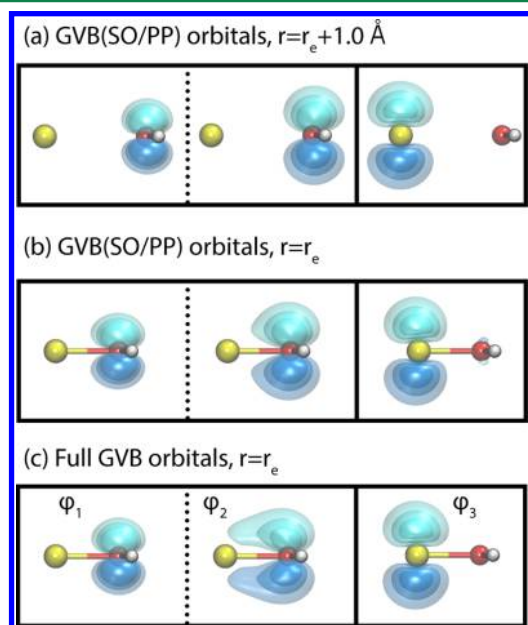


**Figure 6.** (a) GVB(SO/PP) valence  $a''(\pi)$  orbitals at large internuclear separation, (b) GVB(SO/PP) valence  $a''(\pi)$  orbitals at  $r_e$ , and (c) full GVB valence  $a''(\pi)$  orbitals of SOH.

electrons in the two  $a''(\pi)$  orbitals on the oxygen atom are singlet coupled, and the two GVB orbitals have an overlap of 0.87. At  $r_e$ , the oxygen-centered  $2pa''(\pi)$  GVB orbitals remain singlet coupled, and the overlap is essentially the same (0.88); see the GVB(SO/PP) orbitals plotted in Figure 6b. Since strong orthogonality has been imposed, the  $3pa''(\pi)$  sulfur-centered orbital is orthogonal to the two lone pair oxygen orbitals by construction, and the small amount of antibonding character present in this orbital is a result of this constraint.

The full GVB  $a''$  orbitals of SOH at its equilibrium geometry are plotted in Figure 6c. The dominant spin function (98.0%) also singlet couples the electrons in the oxygen-centered orbitals (overlap: 0.83). Thus, there again is no evidence of a recoupled pair bond. However, the unpaired orbital no longer has any antibonding character. Instead, it is clearly localized on the sulfur atom, with overlaps of 0.47 and 0.16 with the two

oxygen lone pair GVB orbitals. These overlaps represent repulsive interactions (Pauli exchange-repulsion<sup>35</sup>) between the electron in the singly occupied sulfur orbital and the pair of electrons in the oxygen-centered orbitals. In effect, the antibonding character of the sulfur-centered  $a''(\pi)$  orbital from the GVB(SO/PP) calculation has been transformed into these unfavorable overlaps.

At  $r_e$ , the overlap of 0.83 between the paired full GVB orbitals on oxygen is somewhat less than in the GVB(SO/PP) wave function. Moreover, instead of slightly increasing upon bond formation as in the GVB(SO/PP) calculation, the overlap decreases. The increase in overlap of the oxygen lone pair orbitals in the GVB(SO/PP) wave function is probably due to the strong orthogonality constraint—the lone pair GVB orbitals must be concentrated more closely together to avoid the sulfur orbital. Nonetheless, the full GVB energy is only 3.5 kcal/mol lower than the GVB(SO/PP) energy, which suggests that the SO and PP approximations are very reasonable for SOH- ( $X^2A''$ ).

For HSO, qualitatively different behavior is observed in the GVB orbitals; see Figure 7. The changes in the GVB(SO/PP)

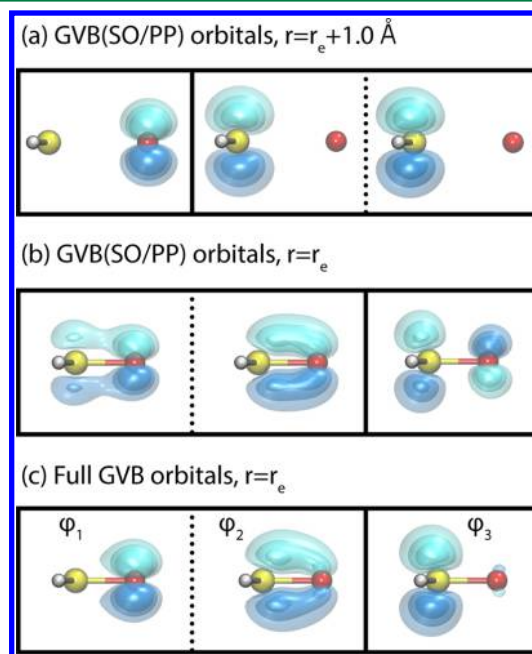


**Figure 7.** (a) GVB(SO/PP) valence  $a''(\pi)$  orbitals at large internuclear separation, (b) GVB(SO/PP) valence  $a''(\pi)$  orbitals at  $r_e$ , and (c) full GVB valence  $a''(\pi)$  orbitals of HSO.

and GVB wave functions as the HS–O distance decreases clearly show the formation of a recoupled pair bond. At  $r(\text{SO}) = r_e(\text{SO}) + 1.0 \text{ \AA}$ , the two electrons on sulfur are singlet coupled with an overlap of 0.88; see Figure 7a. However, at the equilibrium geometry, the GVB(SO/PP) wave function couples the electron in the singly occupied oxygen-centered  $2pa''(\pi)$  orbital with the electron in one of the sulfur-centered lobe orbitals into a singlet pair describing an  $a''(\pi)$  bond. This leaves the remaining electron in a singly occupied orbital that is concentrated on the sulfur atom but polarized away from the bond pair, with substantial antibonding character; see Figure 7b. This orbital is very similar to the singly occupied  $\pi$  orbital in SO shown in Figure 2b. The GVB(SO/PP) orbitals that form the S–O  $a''(\pi)$  bond pair have an overlap of 0.92; the

remaining unpaired orbital has much more antibonding character than the corresponding orbital in the  $\text{SOH}(X^2A'')$  state.

In the full GVB calculations (Figure 7c), we see the same general trends as we observed for SOH: the dominant spin coupling coefficient (89.3%) has the same coupling pattern as the GVB(SO/PP) wave function, the overlap between the bond pair decreases (0.78), and the antibonding character of the unpaired orbital is almost completely absent, being replaced by unfavorable overlaps of 0.62 and 0.18 with the  $a''(\pi)$  bond pair orbitals. These repulsive overlaps are greater than in SOH because the singlet-coupled pair now describes a recoupled pair  $\pi$  bond, the orbitals of which are not as localized as the oxygen lone pair  $\pi$  orbitals of SOH. For HSO, the energy of the full GVB calculation is 12.9 kcal/mol lower than the GVB(SO/PP) calculation. While both sets of orbitals result in the same qualitative conclusions, these results suggest that it may be important to perform full GVB calculations to quantitatively describe the bonding in some sulfur–oxygen compounds. This is consistent with prior studies on sulfur–oxygen compounds by Cooper and co-workers.<sup>36</sup>

In summary, although symmetry constraints mask the formation of a recoupled pair bond in  $\text{SO}(X^3\Sigma^-)$ , we find that in HSO the sulfur-centered  $3p_a''(\pi)^2$  pair—or, rather, the  $(3p_{a_-}, 3p_{a_+})$  lobe orbital pair—is recoupled by the singly occupied oxygen  $2p_a''(\pi)$  orbital, forming a recoupled pair  $a''(\pi)$  bond. As expected, the oxygen  $2p''(\pi)^2$  pair of SOH is not recoupled. As we shall see, the formation of a recoupled pair  $a''(\pi)$  bond is also integral to explaining the differences in bonding between SOO and OSO ( $\text{SO}_2$ ), which has many implications for the energetics and reactivities of these two molecules.

## V. COMPARISON OF THE SOO AND THE OSO ( $\text{SO}_2$ ) ISOMERS

In this section, we consider the addition of an oxygen atom instead of a hydrogen atom to SO to form two structural isomers of sulfur dioxide: the  $X^1A'$  ground state of SOO, where oxygen is the central atom and the  $X^1A_1$  ground state OSO (or  $\text{SO}_2$ ), where sulfur is the central atom. Since oxygen is divalent, there is the possibility of forming both  $\sigma$  and  $\pi$  bonds between SO and the incoming ligand. Orbital diagrams representing these two additions are given in Figure 8.

To form the  $X^1A'$  state of SOO, the incoming oxygen atom forms a  $\sigma$  bond with the oxygen atom of SO. However, as we saw earlier, SO possesses a recoupled pair  $\pi$  bond. This bond must be broken to form the O–O bond, which is expected to

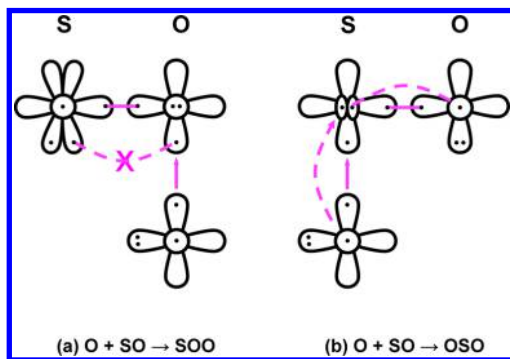


**Figure 8.** GVB orbital diagrams depicting the formation of (a) SOO and (b) OSO ( $\text{SO}_2$ ) by adding an O atom to SO.

weaken the S–O bond as in the formation of the  $X^2A''$  state of SOH. This bonding pattern results in two singly occupied  $\pi$  orbitals localized on the terminal O and S atoms, which leads to substantial diradical character in SOO, similar to what has been previously observed for ozone.<sup>37</sup>

Conversely, in OSO ( $\text{SO}_2$ ), the incoming oxygen atom can form a  $\sigma$  bond with the S atom without disrupting the recoupled pair  $\pi$  bond present in SO, again mirroring the behavior found in the  $X^2A''$  state of HSO. Furthermore, a second SO  $\pi$  bond can be formed with the  $2p\pi$  orbital of the incoming oxygen atom and the unpaired orbital left over from the S–O recoupled pair  $\pi$  bond. This results in the formation of a recoupled pair bond dyad in the  $\pi$  system of  $\text{SO}_2$ .<sup>4</sup>  $\text{SO}_2$  is thus expected to possess little diradical character, as already noted by Glezakou et al.<sup>37</sup> For the remainder of this section, we will refer to this structural isomer simply as OSO to distinguish it from SOO.

**A. Structures and Energetics of the SOO and OSO Isomers.** As we noted above, the SO bond energy of the  $X^2A''$  state of SOH is substantially weaker than in the  $X^3\Sigma^-$  state of SO or the  $X^2A''$  state of HSO because the recoupled pair  $\pi$  bond is disrupted by the formation of the O–H bond. In SOO, the recoupled pair  $\pi$  bond of SO is also broken by formation of an O–O bond. Electron repulsion in the  $\pi$  system is also increased because of the repulsive interaction between the incoming electron in the singly occupied  $\pi$  orbital and the singlet coupled pair of electrons on the central oxygen atom. This leads to longer S–O and O–O bond lengths (1.609 Å and 1.312 Å, respectively) than in the parent diatomic species (1.483 Å for SO and 1.207 Å for  $\text{O}_2$ ). In addition, the S–O bond energy in SOO is just 18.3 kcal/mol, far weaker than the bond energy of  $\text{SO}(X^3\Sigma^-)$  (125.2 kcal/mol) and comparable to the O– $\text{O}_2$  bond strength of ozone, 26.1 kcal/mol.<sup>38</sup> The O–O bond in SOO is also very weak (12.5 kcal/mol).

In OSO, where a recoupled pair  $\pi$  bond dyad is formed, the trends are reversed. The S–O bonds are strengthened and shortened when the second oxygen atom bonds to the sulfur atom. The OS–O bond energy is 133.7 kcal/mol, and the S–O bond length is 1.434 Å. This is consistent with the anticipated bonding pattern. Our previous studies have shown that completing recoupled pair bond dyads yields stronger and shorter bonds.<sup>4</sup>

**B. Analysis of the GVB Wave Functions and Orbitals for SOO and OSO.** The four GVB orbitals for the  $\pi$  system of SOO are shown in Figure 9a. The dominant spin coupling coefficient (>99.9%) singlet couples the two GVB orbitals on the central oxygen atom,  $(\phi_1, \phi_2)$ , with an overlap of 0.80, leaving the GVB orbitals on the terminal atoms,  $(\phi_3, \phi_4)$ , singlet coupled with a small, but non-negligible overlap of 0.15. It is the latter, weak coupling that gives rise to the diradical character of SOO. The bonding in SOO is essentially the same as in the  $X^2A''$  state of SOH. The GVB overlaps of these states are compared in Table 1, where the overlaps from SOO that are analogous to those of SOH (those not involving the  $\pi$  orbital on the terminal oxygen atom) are boxed in green. The GVB descriptions of the two molecules are quite similar but not identical; the SOO overlaps are slightly reduced in magnitude relative to SOH. This is a result of the more diffuse nature of the  $\pi$  system since it is now spread over an additional atom. The  $\pi$  orbitals of SOO are also polarized toward the more electronegative terminal oxygen atom. Therefore, the unfavorable overlaps of the oxygen-centered GVB orbitals are larger



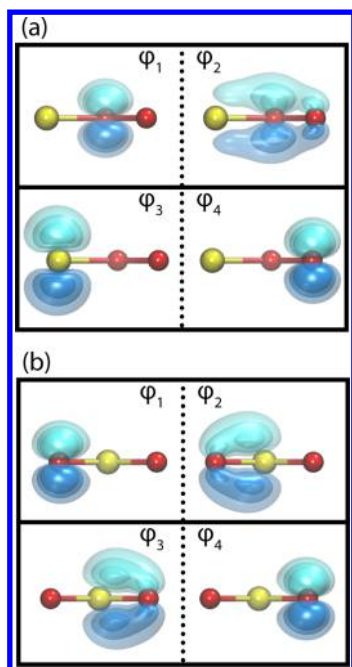


Figure 9. Full GVB valence  $\pi$  orbitals of (a) SOO ( $^1A'$ ) and (b) OSO at  $r_e$ .

Table 1. (a) Overlaps of GVB Orbitals for SOH and (b) Overlaps of GVB Orbitals for SOO<sup>a</sup>

(a)			
	$\varphi_1$	$\varphi_2$	$\varphi_3$
$\varphi_1$	1.00	0.83	0.16
$\varphi_2$		1.00	0.47
$\varphi_3$			1.00

(b)				
	$\varphi_1$	$\varphi_2$	$\varphi_3$	$\varphi_4$
$\varphi_1$	1.00	0.80	0.11	0.21
$\varphi_2$		1.00	0.42	0.43
$\varphi_3$			1.00	0.15
$\varphi_4$				1.00

<sup>a</sup>Favorable overlaps in the dominant spin-coupling pattern are given in blue, and unfavorable overlaps are in red.

(0.43 and 0.21) than those of the sulfur atom and the central oxygen atom (0.42 and 0.11).

The bonding in OSO is qualitatively different than in SOO; the dominant spin-coupling coefficient (98.9%) contains two  $\pi$  bonds with favorable overlaps of 0.71. The overlap between the two GVB orbitals (shown in Figure 9b) on the central atom, ( $\phi_2$ ,  $\phi_3$ ), is now unfavorable but reduced to 0.46 (relative to 0.89 in the sulfur atom). The overlap between the two terminal GVB orbitals, ( $\phi_1$ ,  $\phi_4$ ), is also unfavorable but is just 0.06. The

shortening and strengthening of the OSO bonds relative to SO is a direct result of the formation of the recoupled pair bond dyad and the reduction in the unfavorable orbital overlaps. The relevant overlap comparison is shown in Table 2a and in the

Table 2. (a) Overlaps of GVB Orbitals for HSO and (b) Overlaps of GVB Orbitals for SO<sub>2</sub><sup>a</sup>

(a)			
	$\varphi_1$	$\varphi_2$	$\varphi_3$
$\varphi_1$	1.00	0.78	0.18
$\varphi_2$		1.00	0.62
$\varphi_3$			1.00

(b)				
	$\varphi_1$	$\varphi_2$	$\varphi_3$	$\varphi_4$
$\varphi_1$	1.00	0.71	0.09	0.06
$\varphi_2$		1.00	0.46	0.09
$\varphi_3$			1.00	0.71
$\varphi_4$				1.00

<sup>a</sup>Favorable overlaps in the dominant spin-coupling pattern are given in blue, and unfavorable overlaps are in red.

boxed values in Table 2b. In the  $X^2A''$  state of HSO, where the unpaired electron is not forming any bonds, the unfavorable overlaps are 0.62 and 0.18. In OSO, however, the electron left over from formation of the recoupled pair  $\pi$  bond is bonded to a singly occupied  $\pi$  orbital of the second oxygen atom, which results in its delocalization onto that oxygen atom. This reduces the unfavorable overlaps to 0.46 and 0.09. Formation of this bond reduces the favorable overlap from 0.78 to 0.71, but the formation of an additional bond and the reduction of the unfavorable overlaps more than compensates for this decrease.

It is worth noting that these results are in basic agreement with prior GVB studies of sulfur dioxide. Unpublished GVB(SO/PP) calculations by one of the authors (T.H.D.) in the early 1980s also showed the formation of two  $\pi$  bonds. Improving on these results by removing the perfect pairing and, more importantly, removing the strong orthogonality constraints, we find orbitals that also describe a  $\pi$  bonded structure, essentially providing OSO with two S–O double bonds. Cooper et al.<sup>36</sup> also performed full GVB (SCVB) calculations on the  $\pi$  system of OSO, although including different orbitals in the active space. Our results are in good agreement with theirs. The current work adds to this collection of studies by interpreting the orbitals and rationalizing the differences in bonding with GVB theory and the recoupled pair bonding model. The differences in the structure and energetics of the SOO and OSO provide compelling additional evidence for the presence of a recoupled pair  $\pi$  bond in  $SO(X^3\Sigma^-)$  and dramatically illustrates the effects of recoupled pair bonds and dyads.

## VI. CONCLUSION

The GVB wave function provides unrivaled insights into the nature of bonding in molecules and a clear description of a new type of bond that can be formed by the elements in the second and subsequent rows of the periodic table—the *recoupled pair bond*. GVB calculations help elucidate the role of recoupled pair bonds and recoupled pair bond dyads in determining the structure, energetics, and reactivities of molecules containing these elements. In this paper, we used detailed GVB calculations to obtain insights into the remarkable differences between the HSO and SOH isomers and extended these results to account for the differences between SOO and OSO.

A recoupled pair  $\pi$  bond exists in the ground state of  $\text{SO}(\text{X}^3\Sigma^-)$ , but its presence is masked by symmetry considerations. The presence of the recoupled pair  $\pi$  bond in SO was revealed by lowering the symmetry, namely, adding a hydrogen atom to SO to form HSO and SOH. The recoupled pair  $\pi$  bond persists in HSO but must be broken to form SOH, which accounts for the surprising lengthening and weakening of the SO bond in the ground state of SOH relative to that of HSO. The GVB orbitals of the  $\pi$  system of these molecules possess qualitative differences in their orbital coupling patterns that reflect the presence (HSO) or absence (SOH) of a recoupled pair bond. The results presented here are consistent with prior MO-based calculations on HSO and SOH, although our use of the GVB wave function allows us to gain more detailed insights into the description of bonding in these species. For example, a prior NBO analysis of the HSO and SOH wave functions showed a greater degree of  $\pi$  bonding in the former, and recoupled pair bonding explains why this is so.<sup>39</sup> Further, these authors note the small dissociation energy (88.1 kcal/mol) computed for the OH bond in SOH by subtracting the energy of  $\text{SOH}(\text{X}^2\text{A}')$  from that of  $\text{H}^1\text{S} + \text{SO}(\text{X}^3\Sigma^-)$ . While this result alone could be due to any number of factors (poor overlap of the O and H atoms or steric repulsion with the incoming hydrogen atom, for instance), our analysis presents a clear explanation for this finding: the presence of the recoupled pair  $\pi$  bond in SO but not in SOH. The small energy difference between HSO and SOH can be understood as a near cancellation of two effects: (1) the inherently greater strength of an OH bond versus an SH bond, which favors SOH over HSO, and (2) the energetics gains from the presence of the recoupled pair bond in HSO but not in SOH, which favors HSO over SOH.

The same “veiled” recoupled pair  $\pi$  bond in  $\text{SO}(\text{X}^3\Sigma^-)$  also explains the differences in the lengths and strengths of the bonds in SOO and OSO ( $\text{SO}_2$ ). The orbital left over from formation of the recoupled pair  $\pi$  bond in SO is concentrated on the sulfur atom. Therefore, an incoming divalent ligand, such as an oxygen atom, approaching the sulfur atom can form both a  $\sigma$  and a  $\pi$  bond to form  $\text{SO}_2$ . The new  $\pi$  bond strengthens the SO bonds, explaining why the bonds in  $\text{SO}_2$  are shorter and stronger than the bond in the SO diatomic molecule. However, in the converse situation where a divalent ligand bonds with the oxygen atom of SO, the recoupled pair  $\pi$  bond is broken, and there is no longer the possibility of forming a second  $\pi$  bond. The net result is a substantially longer and weaker SO bond in SOO than in either  $\text{SO}_2$  or SO. As a result, SOO has substantial diradical character and is much less stable than the OSO isomer.

The results presented here further demonstrate the utility of the GVB wave function and recoupled pair bonding model in

explaining the rather dramatic differences in structure and energetics of two isoelectronic sulfur–oxygen compounds. Not only does recoupled pair bonding successfully rationalize these differences, but the results of the calculations are in agreement with the *predictions* made from GVB diagrams. We expect that the findings presented here apply generally to sulfur–oxygen compounds where a doubly occupied sulfur orbital can be aligned with a singly occupied oxygen orbital, and ongoing calculations in our group support the notion that recoupled pair bonding of  $\pi$  electrons should be considered when short SO bonds are observed.

## ■ ASSOCIATED CONTENT

### Supporting Information

Optimized geometries and absolute energies for all species ( $\text{X}^2\text{A}''$  and  $\text{A}^2\text{A}'$  states of HSO and SOH,  $\text{X}^1\text{A}'$  state of SOO, and  $\text{X}^1\text{A}_1$  state of OSO) presented in this work. This material is available free of charge via the Internet at <http://pubs.acs.org>.

## ■ AUTHOR INFORMATION

### Corresponding Author

\*E-mail: [thdjr@illinois.edu](mailto:thdjr@illinois.edu).

### Notes

The authors declare no competing financial interest.

## ■ ACKNOWLEDGMENTS

This work was supported by the Distinguished Chair for Research Excellence in Chemistry and the National Center for Supercomputing Applications at the University of Illinois at Urbana–Champaign. One of the authors (B.A.L.) is the grateful recipient of a National Science Foundation Graduate Research Fellowship.

## ■ REFERENCES

- (1) Wilson, A. K.; Dunning, T. H. *J. Phys. Chem. A* **2004**, *108*, 3129–3133.
- (2) Purser, G. H. *J. Chem. Educ.* **1999**, *76*, 1013–1018.
- (3) Chen, L.; Woon, D. E.; Dunning, T. H. *J. Phys. Chem. A* **2009**, *113*, 12645–12654.
- (4) Dunning, T. H., Jr.; Woon, D. E.; Leiding, J.; Chen, L. *Acc. Chem. Res.* **2013**, *46*, 359–368.
- (5) Leiding, J.; Woon, D. E.; Dunning, T. H. *J. Phys. Chem. A* **2011**, *115*, 4757–4764.
- (6) Leiding, J.; Woon, D. E.; Dunning, T. H. *J. Phys. Chem. A* **2011**, *115*, 329–341.
- (7) Woon, D. E.; Dunning, T. H. *J. Phys. Chem. A* **2009**, *113*, 7915–7926.
- (8) Woon, D. E.; Dunning, T. H. *Mol. Phys.* **2009**, *107*, 991–998.
- (9) Woon, D. E.; Dunning, T. H. *J. Phys. Chem. A* **2010**, *114*, 8845–8851.
- (10) Barnes, I.; Hjorth, J.; Mihalopoulos, N. *Chem. Rev. (Washington, DC, U. S.)* **2006**, *106*, 940–975.
- (11) Tyndall, G. S.; Ravishankara, A. R. *Int. J. Chem. Kinet.* **1991**, *23*, 483–527.
- (12) Zhang, S. S.; Foster, D.; Read, J. J. *Power Sources* **2010**, *195*, 3684–3688.
- (13) Lee, Y. Y.; Lee, Y. P.; Wang, N. S. *J. Chem. Phys.* **1994**, *100*, 387–392.
- (14) Lovejoy, E. R.; Wang, N. S.; Howard, C. J. *J. Phys. Chem.* **1987**, *91*, 5749–5755.
- (15) Wang, N. S.; Howard, C. J. *J. Phys. Chem.* **1990**, *94*, 8787–8794.
- (16) Goddard, W. A.; Dunning, T. H.; Hunt, W. J.; Hay, P. J. *Acc. Chem. Res.* **1973**, *6*, 368–376.
- (17) Hiberty, P. C.; Shaik, S. J. *Comput. Chem.* **2007**, *28*, 137–151.



- (18) Bobrowicz, F. W.; Goddard, W. A. In *Modern Theoretical Chemistry*; Schaefer, H. F., Ed.; Plenum: New York, 1977; Vol. 3, p 79.
- (19) Werner, H. J.; Knowles, P. J.; Knizia, G.; Manby, F. R.; Schutz, M.; Celani, P.; Korona, T.; Lindh, R.; Mitrushenkov, A.; Rauhut, G.; Shamasundar, K. R.; Adler, T. B.; Amos, R. D.; Bernhardsson, A.; Berning, A.; Cooper, D. L.; Deegan, M. J. O.; Dobbyn, A. J.; Eckert, F.; Goll, E.; Hampel, C.; Hesselmann, A.; Hetzer, G.; Hrenar, T.; Jansen, G.; Koppl, C.; Liu, Y.; Lloyd, A. W.; Mata, R. A.; May, A. J.; McNicholas, S. J.; Meyer, W.; Mura, M. E.; Nicklass, A.; O'Neill, D. P.; Palmieri, P.; Pflüger, K.; Pitzer, R.; Reiher, M.; Shiozaki, T.; Stoll, H.; Stone, A. J.; Tarroni, R.; Thorsteinsson, T.; Wang, M.; Wolf, A. *MOLPRO*, version 2010.1; Cardiff University: Cardiff, U. K.; Universität Stuttgart: Stuttgart, Germany, 2010. See <http://molpro.net>.
- (20) Thorsteinsson, T.; Cooper, D. L.; Gerratt, J.; Karadakov, P. B.; Raimondi, M. *Theor. Chim. Acta* **1996**, 93, 343–366.
- (21) Cooper, D. L.; Thorsteinsson, T.; Gerratt, J. *Int. J. Quantum Chem.* **1997**, 65, 439–451.
- (22) Knowles, P. J.; Werner, H. J. *Chem. Phys. Lett.* **1985**, 115, 259–267.
- (23) Werner, H. J.; Knowles, P. J. *J. Chem. Phys.* **1985**, 82, 5053–5063.
- (24) Knizia, G.; Adler, T. B.; Werner, H. J. *J. Chem. Phys.* **2009**, 130, 054104.
- (25) Knizia, G.; Werner, H. J. *J. Chem. Phys.* **2008**, 128, 154103.
- (26) Knowles, P. J.; Hampel, C.; Werner, H. J. *J. Chem. Phys.* **1993**, 99, 5219–5227.
- (27) Manby, F. R. *J. Chem. Phys.* **2003**, 119, 4607–4613.
- (28) Adler, T. B.; Knizia, G.; Werner, H. J. *J. Chem. Phys.* **2007**, 127, 221106.
- (29) Dunning, T. H. *J. Chem. Phys.* **1989**, 90, 1007–1023.
- (30) Woon, D. E.; Dunning, T. H. *J. Chem. Phys.* **1993**, 98, 1358–1371.
- (31) Dunning, T. H.; Peterson, K. A.; Wilson, A. K. *J. Chem. Phys.* **2001**, 114, 9244–9253.
- (32) Hund, F. Z. *Phys.* **1928**, 51, 759–795.
- (33) Huber, K. P.; Herzberg, G. *Molecular Spectra and Molecules. IV. Constants of Diatomic Molecules*; Van Nostrand: Princeton, NJ, 1979.
- (34) Cordero, B.; Gomez, V.; Platero-Prats, A. E.; Reves, M.; Echeverria, J.; Cremades, E.; Barragan, F.; Alvarez, S. *Dalton Trans.* **2008**, 2832–2838.
- (35) Pauli, W. Z. *Phys.* **1925**, 31, 765–783.
- (36) Cunningham, T. P.; Cooper, D. L.; Gerratt, J.; Karadakov, P. B.; Raimondi, M. J. *Chem. Soc., Faraday Trans.* **1997**, 93, 2247–2254.
- (37) Glezakou, V. A.; Elbert, S. T.; Xantheas, S. S.; Ruedenberg, K. J. *Phys. Chem. A* **2010**, 114, 8923–8931.
- (38) Chase, M. W.; Davies, C. A.; Downey, J. R.; Frurip, D. J.; McDonald, R. A.; Syverud, A. N. *J. Phys. Chem. Ref. Data* **1985**, 14, 1–926.
- (39) Perez-Juste, I.; Carballeira, L. *J. Mol. Struct.: THEOCHEM* **2008**, 855, 27–33.